Radiation of spin waves from the open end of a microscopic magnetic-film waveguide

Vladislav E. Demidov,[1,*] Sergej O. Demokritov,[1] Daniel Birt,[2,3] Brian O'Gorman,[2] Maxim Tsoi,[2,3] and Xiaoqin Li[2,3]
[1]*Institute for Applied Physics, University of Muenster, Corrensstrasse 2-4, 48149 Muenster, Germany*
[2]*Department of Physics, Center for Nano- and Molecular Science and Technology, University of Texas at Austin, Austin, Texas 78712, USA*
[3]*Texas Materials Institute, University of Texas at Austin, Austin, Texas 78712, USA*
(Received 25 May 2009; published 27 July 2009)

We have studied experimentally the radiation of spin waves from a permalloy-film microwaveguide into a continuous permalloy film. We show that due to a strong mismatch of the spin-wave spectrum caused by a variation in the demagnetizing field at the interface between the waveguide and the film, a frequency interval exists, where spin waves experience total reflection from the junction penetrating into the permalloy film in a tunnelinglike manner. At frequencies above this interval, complex frequency-dependent radiation patterns were observed characterized by a preferential radiation direction appearing due to the intrinsic anisotropy of the spin-wave dispersion characteristics in the film.

DOI: 10.1103/PhysRevB.80.014429 PACS number(s): 75.30.Ds, 75.40.Gb, 75.75.+a, 85.75.−d

I. INTRODUCTION

The propagation of spin waves in microscopic waveguiding structures has recently started to attract considerable attention in connection with their potential applications for integrated signal processing.[1–16] With recent developments in nanoscale patterning techniques and the experimental methods enabling characterization of spin-wave propagation in microscopic guiding structures, in addition to the numerous theoretical activities in this field,[1–4,7,14,15] a series of experimental studies were reported.[5,6,8–13,16,17] These investigations have shown that even relatively simple magnetic-film structures can demonstrate a large number of remarkable spin-wave-propagation phenomena interesting from the point of view of technical applications, as well as from the point of view of fundamental physics. This richness is due to the very specific combination of confinement and demagnetizing effects, a unique intrinsic anisotropy of the spin-wave dispersion characteristics, and their controllability by the magnetic field. As was recently shown,[16] the joint action of these factors not only provides a way for realization of different signal-processing operations, but also leads to unusual basic nonlinear phenomena which do not appear on the macroscopic scale.

Among topics that are of general interest in the physics of waves of different nature, the question of wave transformations at a junction between a spatially confined waveguiding element and an unconfined medium is of particular importance. For spin waves in microscopic structures, such a junction is expected to demonstrate transformations that cannot be observed for other types of waves because of spatial variations of the demagnetizing field and strong in-plane anisotropy of spin-wave characteristics. Recently, it was demonstrated[13] that these phenomena strongly affect the spin-wave propagation even in the case of a gradual variation in the width of a microscopic stripe waveguide leading to a large number of different transformation patterns. Therefore, one should expect nontrivial radiation characteristics at the interface between a confined waveguide and an unconfined film. Such a junction was recently used in Ref. 18 to study spin-wave interference effects, but particular features of spin-wave radiation in the system were not analyzed in this previous work.

Here we report on the experimental investigations of spin-wave radiation from a 2-μm-wide magnetic-stripe waveguide into a continuous magnetic film. The measurements were performed using spatially resolved microfocus Brillouin light scattering (μBLS) spectroscopy, which allowed the direct two-dimensional visualization of spin-wave propagation with the submicrometer spatial resolution. We show that the radiation of spin waves is strongly affected by the spatial variations of the demagnetizing field. These variations lead to a total reflection of spin waves if their frequency lies within a certain interval. At frequencies where the radiation is allowed, one observes rather unusual propagation features originating from the anisotropy of the spin-wave dispersion. The spin-wave patterns exhibit a multiple-ray structure with a clearly defined preferential radiation direction depending on the excitation frequency and the static magnetic field. We also provide an analytical model explaining these experimental findings.

II. EXPERIMENT

Figure 1 shows the sketch of samples used in the experiments. A 36-nm-thick permalloy (Py) film deposited onto a sapphire substrate by a magnetron sputtering was patterned using a focused ion beam to define a 2-μm-wide and 20-μm-long stripe waveguides, as shown in the figure. After the patterning process, the structure was covered by a 5-nm-thick SiO_2 layer to provide protection from oxidation and electrical isolation of the Py structure from the excitation circuit. Finally, a 150-nm-thick gold (Au) stripe antenna was defined using photolithography followed by thermal deposition of the gold and a lift-off process. The antenna had a width of $t=2.4$ μm and was positioned at a distance of 3.2 μm from the junction between the stripe waveguide and the unpatterned film. The sample was placed into a uniform static magnetic field $H_0=900$ Oe applied in the plane of the Py waveguide and perpendicular to its axis. In this way, the

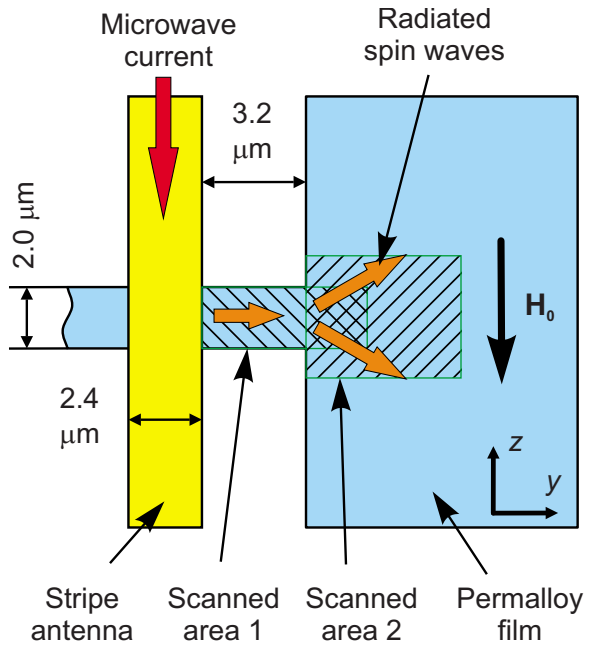

FIG. 1. (Color online) Sketch of the samples.

propagation geometry of the so-called Damon-Eshbach (DE) spin waves[19] was realized for the waveguide.

The excitation of spin waves was performed by a transmission through the stripe antenna of a continuous-wave microwave current at a fixed frequency F. The current created a dynamic magnetic field h coupled to the dynamic magnetization in the permalloy waveguide mainly via its in-plane component h_y, providing a well-localized excitation of spin waves underneath the antenna. Due to the finite width of the antenna, spin waves with wave numbers up to the order of magnitude of $\pi/t \approx 1$ μm^{-1} can be effectively excited in the waveguide. The detection of spin waves was performed by the μBLS technique described in detail elsewhere.[20] Using this technique we mapped two-dimensional spatial distributions of the spin-wave intensity with submicrometer resolution. In particular, two spatial regions were analyzed: the part of the waveguide between the antenna and the continuous film (scanned area 1 in Fig. 1) and the part of the continuous film adjacent to the junction with the waveguide (scanned area 2 in Fig. 1).

Before analyzing experimental results, we briefly review the theoretical background of spin-wave propagation in the system under investigation. Figure 2 shows the spin-wave dispersion characteristics for the stripe waveguide and the continuous magnetic film calculated for our experimental conditions using the theory developed in Ref. 21. The curve marked in Fig. 2 as "waveguide mode" is the dispersion curve for the fundamental mode in the 2-μm-wide waveguide calculated according to Ref. 9. This mode has the simplest half-sine distribution of the spin-wave amplitude over the waveguide width and is characterized by the transverse wave number $k_z = \pi/w$, where w is the width of the waveguide. Higher order modes[9] with $k_z = n\pi/w$, $n > 1$ are not considered here, because, as follows from the experimental data, they are excited by the used antenna very inefficiently. The lines labeled with $\theta = 0$, 30, 45, and 90° are the spin-

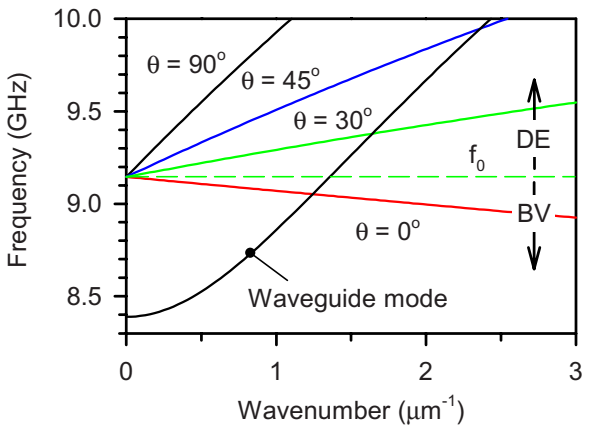

FIG. 2. (Color online) Dispersion characteristics of spin waves in the waveguide (waveguide mode) and the continuous permalloy film calculated for the conditions of the experiment. θ is the angle between the direction of the static magnetic field and the wave vector of spin waves in the continuous film. f_0 is the frequency of the uniform ferromagnetic resonance.

wave dispersion curves calculated for the continuous film for different angles θ between the direction of the static magnetic field and the wave vector of spin waves [$\theta = \arctan(k_y/k_z)$]. In contrast to spin waves in the waveguide, for which only discrete values of k_z are allowed ($k_z = n\pi/w$), every combination of k_y and k_z is allowed for spin waves in the film. The horizontal dashed line in Fig. 2 marks the frequency of the uniform ferromagnetic resonance f_0 in the film, which separates the frequency regions of DE and backward volume (BV) spin waves.

As seen from Fig. 2, the spectrum of spin waves in the waveguide is shifted with respect to that in the continuous film toward smaller frequencies. This happens due to the reduction in the internal magnetic field caused by the demagnetizing effects in the waveguide.[13] Note that spin waves of the fundamental waveguide mode have a lower cutoff frequency at $k_y = 0$. It is equal to about 8.4 GHz for our experimental conditions. The lower cutoff frequency of the spin-wave spectrum in the film is 8.3 GHz corresponding to $k_y \approx 25.6$ μm^{-1} (out of the range of Fig. 2). Such a mismatch between the spectra results in a significant conversion of the wave vector of spin waves radiated from the waveguide into the film. However, the interval of wave numbers where this conversion is possible is much smaller than 25.6 μm^{-1}. In fact, it is determined by the waveguide width, which defines the scale where the translational symmetry of the unconfined film is broken. Thus, the radiation of spin waves with $k_y \gg \pi/w = 1.5$ μm^{-1}, i.e., with the frequency much below 9 GHz, happens very inefficiently. Correspondingly, the mismatch between two spectra results in the appearance of a frequency range between the lower cutoff frequency of the waveguide mode at 8.4 GHz and about 9 GHz where spin-wave propagation is allowed for the confined waveguide, but their radiation into the continuous film is very unlikely. For larger frequencies, the above discussed conversion is allowed. However, it is accompanied by a noticeable change in the wave vector of spin waves. Therefore, one can expect nontrivial frequency-dependent radiation characteristics.

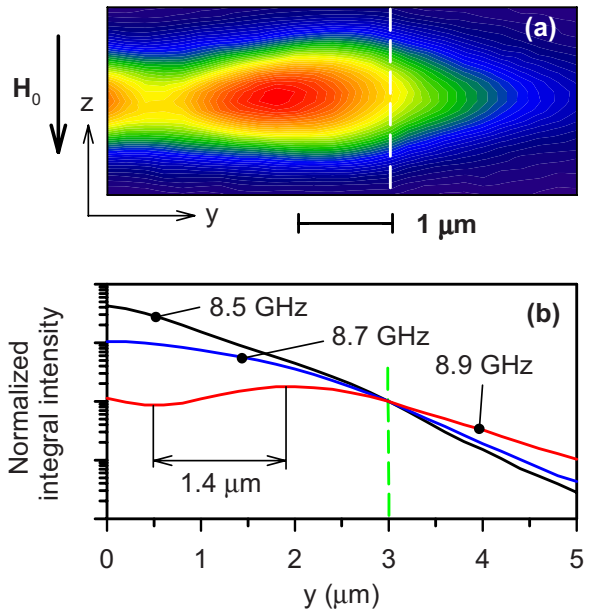

FIG. 3. (Color online) (a) Spin-wave intensity map corresponding to area 1 in Fig. 1 recorded for the excitation frequency $F=8.9$ GHz. The map has dimensions of 2×5 μm in the z and y directions, respectively. The vertical dashed line shows the position of the junction between the waveguide and the continuous film. (b) Spin-wave intensity integrated over transverse cross sections of the stripe waveguide as a function of the propagation coordinate for three different excitation frequencies as indicated. The data are normalized at the position of the junction. Note the logarithmic scale of the vertical axis.

III. RESULTS AND DISCUSSION

In the first step of the experiments, we analyzed the propagation of spin waves within the frequency range where the radiation is prohibited. For this, we measured two-dimensional maps of the spin-wave intensity in the spatial area 1 (see Fig. 1) for F gradually increasing from 8.4 GHz. A typical spin-wave intensity map obtained in these measurements is shown in Fig. 3(a). The map has dimensions of 2×5 μm and was recorded with spatial step sizes of 0.1 and 0.2 μm in the z and y directions, respectively. The vertical dashed line in Fig. 3(a) shows the position of the junction between the waveguide and the continuous film. Figure 3(a) proves the absence of the spin-wave radiation within the discussed frequency range. On the right side from the position of the junction the spin waves exhibit very fast decay of their intensity. On the left side they show a nonmonotonous dependence of the intensity on the propagation coordinate y with a clear maximum and a minimum caused by a formation of a standing wave. Figure 3(b) further characterizes the spin-wave behavior at different frequencies. It shows dependencies of the spin-wave intensity integrated over transverse cross sections of the waveguide on the propagation coordinate for three different excitation frequencies. The integrated intensity is normalized at the position of the junction. As seen from Fig. 3(b), the decay of the spin-wave intensity in the continuous film is nearly exponential (note the logarithmic scale) and slightly weakens with the increase in the frequency. Within the waveguide, the intensity profile shows a behavior typical for the formation of a standing wave. At the frequency of 8.9 GHz, one can clearly see its node at $y=0.5$ μm. By measuring the distance from this node to the nearest maximum, one can estimate the wavelength of spin waves λ. As seen from Fig. 3(b), $\lambda/4=1.4$ μm, which agrees well with the theoretical value of 1.47 μm calculated based on the spin-wave spectrum shown in Fig. 2. Note that since the wavelength of the standing wave should increase with decreasing frequency, the corresponding minima are not seen for lower frequencies.

Considering the discussion of the data in Fig. 3, one concludes that the shift of the spin-wave spectrum due to the variation in the demagnetizing field leads to total spin-wave reflection from the junction between the waveguide and the continuous film with the formation of a standing spin wave inside of the waveguide. The reflection is accompanied by a tunnelinglike[22] penetration of the spin wave into the continuous film. The penetration length appears to increase with increasing frequency (decreasing wavelength) of the incident spin wave. This does not allow one to directly relate the penetration length to the spin-wave wavelength, as one expects for a nonresonant excitation by a dipole field. Most probably the found dependence is caused by the frequency-dependent dynamic susceptibility of the permalloy film, which increases as the frequency approaches the frequency of the uniform resonance f_0.

As discussed above, increasing the frequency F one should finally come to the situation when the radiation of spin waves into the continuous film becomes allowed. Experimentally we detected the appearance of the radiation for $F>9$ GHz, which agrees with the estimations presented in the previous section. Since the observed radiation has rather complex character we need to discuss the peculiarities of spin-wave dispersion in a continuous ferromagnetic film first. Figure 4 shows another representation of the spin-wave spectrum shown in Fig. 2. The lines in Fig. 4 are the constant-frequency contours projected onto the k_y-k_z plane. In this representation, the vector of the phase velocity $\mathbf{V}_{\mathrm{ph}}$ is parallel to the wave vector $\mathbf{k}=(k_y,k_z)$, whereas the vector of the group velocity $\mathbf{V}_g$ is directed along the normal to the constant-frequency contour $[\mathbf{V}_g=2\pi\nabla F(k_y,k_z)]$. Figure 4 shows that the dispersion characteristics of spin waves have very specific anisotropy: while the direction of the phase velocity for a given frequency can change in a wide range of angles (as usual for sound and light waves), the group velocity exhibits a certain preferential direction only slightly dependent on F and the type of spin waves (DE or BV). The transformation of spin waves at the interface between the stripe waveguide and the continuous film can be considered as a reradiation that conserves the frequency, but not the wave vector. In this case, the spin waves radiated into the continuous film should have all combinations of k_y and k_z possible for the given F, limited by the inefficiency of the wave vector conversion only. Nevertheless, despite this large diversity in the direction of the phase velocity, the radiated waves should show a preferential direction of the energy flow defined by the direction of the group velocity.[23] This fact is further illustrated by Fig. 5, which shows dependencies of the angle of the group velocity α with respect to the

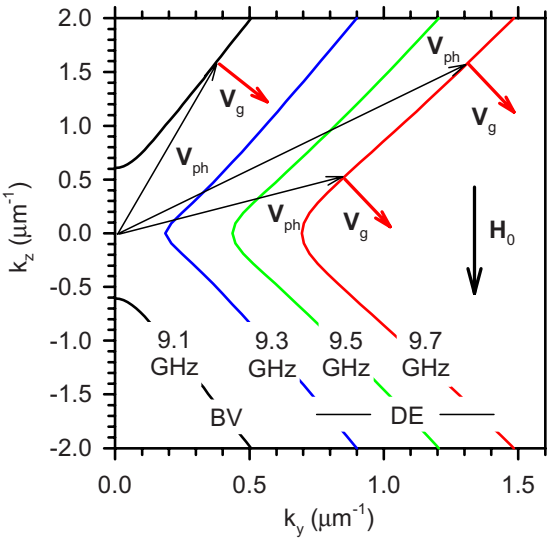

FIG. 4. (Color online) Dispersion characteristics of spin waves in a continuous magnetic film in the form of projection of constant-frequency contours onto the k_y-k_z plane. Arrows show the directions of the phase $\mathbf{V}_{ph}$ and group $\mathbf{V}_g$ velocities. $\mathbf{H}_0$ is the direction of the static magnetic field.

direction of the static magnetic field on the component of the wave vector k_z for different spin-wave frequencies. As seen from Fig. 5, with the increase in k_z the angle α quickly saturates at a value close to 70° and then stays nearly constant. As a result, this direction is expected to dominate over others in the radiation process. The inset in Fig. 5 shows the frequency variation of the mean angle α for the interval of $k_z = 1-3$ μm^{-1}, where the dependencies of Fig. 5 are saturated. These data can be directly used for comparison with the experimental results.

Figure 6 presents the experimentally obtained maps of spin-wave radiation at frequencies higher than the radiation threshold 9.0 GHz. The maps correspond to the area 2 in Fig.

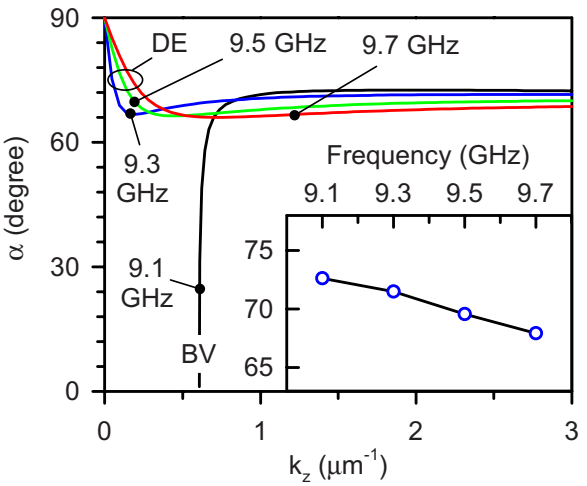

FIG. 5. (Color online) Dependencies of the angle of the group velocity α with respect to the direction of the static magnetic field on the component of the wave vector k_z for different spin-wave frequencies as indicated. Inset—frequency variation of the mean angle α for the interval of $k_z = 1-3$ μm^{-1}.

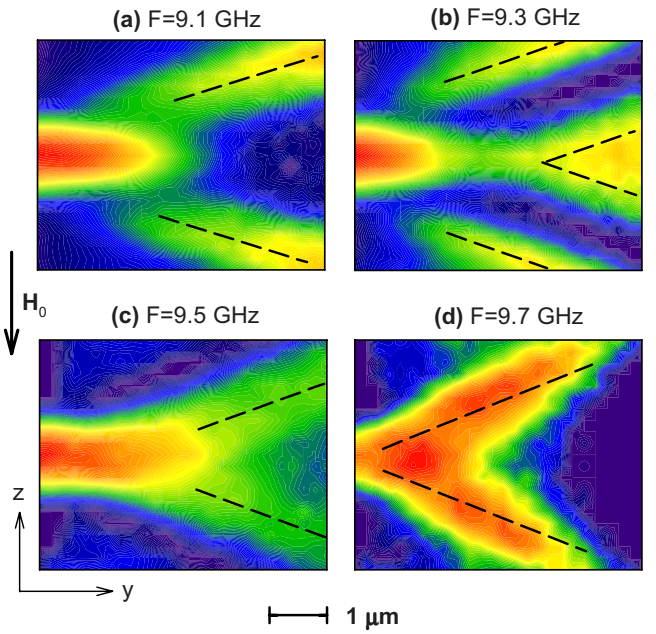

FIG. 6. (Color online) Experimentally obtained maps of the spin-wave radiation at different frequencies as indicated. The maps correspond to area 2 in Fig. 1 and have dimensions of 4×5 μm in the z and y directions, respectively. The spatial decay of spin waves is numerically compensated. Dashed lines show the theoretically obtained directions of preferential radiation.

1 and have dimensions of 4×5 μm in the z and y directions, respectively. They were recorded with a spatial step size of 0.2 μm. To elucidate the intrinsic structure of the radiation patterns, the spatial decay of spin waves is numerically compensated by normalizing the integral of the spin-wave intensity over the z sections of the maps.[13] Figure 6 clearly shows that, in accordance with the above theoretical discussion, the radiation of spin waves into the continuous film happens along certain clearly defined directions only, resulting in a formation of spin-wave rays oriented at a certain angle with respect to the direction of the static magnetic field $\mathbf{H}_0$. To compare the experimental data with the theory, we draw dashed lines on top of the spin-wave rays in Fig. 6 with the angles to the direction $\mathbf{H}_0$ taken from the inset of Fig. 5. This comparison shows that the theory predicts the radiation angle with very good accuracy. In fact, the experimentally obtained angle deviates noticeably from the calculated one only for the highest accessible frequency of 9.7 GHz. The reason for the reduced propagation angle is not clear at the moment. The experimentally found angle α for the pattern in Fig. 6(d) is equal to about 56°, which is smaller than the minimum angle obtained from the theoretical spin-wave dispersion spectrum for $F = 9.7$ GHz (see Fig. 5). Therefore, this effect cannot be associated with small modifications of the spectrum due to anisotropy or nonuniformity of the internal magnetic field.

Another interesting feature of the spin-wave radiation seen in Fig. 6 is the strong dependence of the intrinsic structure of the radiation pattern on the excitation frequency. Though all the maps in Fig. 6 demonstrate a preferential radiation direction in agreement with the theory, the number

of spin-wave rays and their spatial positions can change. We associate this fact with a nonlocal character of the dipolar magnetic fields produced by the spin waves. As was shown above, these long-range fields lead to a significant penetration of spin waves into the continuous film, even in the regime of the total reflection. In the radiation regime they cause a strong nonadiabaticity of the spin-wave conversion process at the junction between the waveguide and the continuous film. Since the influence of the dipolar fields is weaker for short-wavelength spin waves, one expects a simplification of the structure of the radiation patterns with the increase in the frequency. This is in agreement with the data of Fig. 6. For small frequencies [see Figs. 6(a) and 6(b)] the radiation patterns demonstrate a tail of the waveguide mode caused by its dipolar fields similar to that seen in Fig. 3(a). This tail serves as a radiation source for two or even four spin-wave rays. At higher frequencies [see Figs. 6(c) and 6(d)], the tail of the waveguide mode becomes less pronounced and the radiated rays start directly at the position of the junction between the waveguide and the continuous film.

IV. CONCLUSIONS

Our experimental results show that in microscopic magnetic-film structures the spin-wave transformations at the junction between a patterned stripe waveguide and the continuous film have rather complex character because of the spatial variation of the demagnetizing fields and the specific anisotropy of the spin-wave dispersion characteristics. A simple analytical model can be used to describe the qualitative characteristics of the spin-wave radiation in such systems, but a deeper understanding of its particular properties demands the development of a more complete theory or numerical simulations. We believe that our experimental findings will stimulate such developments in the future.

Note added in proof. Recently, our attention was drawn to Ref. 24, where a similar geometry, albeit with macroscopic dimensions, was investigated.

ACKNOWLEDGMENTS

The work in Muenster was supported in part by the Deutsche Forschungsgemeinschaft. The work in Texas was supported in part by the following agencies: AFOSR under Grants No. FA9550-08-1-0463 and No. FA-9550-08-1-0058, Texas-ARP under Grant No. 003658-0160-2007, the Alfred P. Sloan Foundation, and the University of Texas. D.B. gratefully acknowledges support from the NSF-IGERT program via Grant No. DGE-0549417.

*Corresponding author; demidov@uni-muenster.de

[1] A. Khitun, R. Ostroumov, and K. L. Wang, Phys. Rev. A **64**, 062304 (2001).
[2] R. Hertel, W. Wulfhekel, and J. Kirschner, Phys. Rev. Lett. **93**, 257202 (2004).
[3] S. Choi, K.-S. Lee, K. Yu. Guslienko, and S.-K. Kim, Phys. Rev. Lett. **98**, 087205 (2007).
[4] H. Xi and S. Xue, J. Appl. Phys. **101**, 123905 (2007).
[5] M. P. Kostylev, G. Gubbiotti, J.-G. Hu, G. Carlotti, T. Ono, and R. L. Stamps, Phys. Rev. B **76**, 054422 (2007).
[6] V. E. Demidov, S. O. Demokritov, K. Rott, P. Krzysteczko, and G. Reiss, Appl. Phys. Lett. **92**, 232503 (2008).
[7] K.-S. Lee and S.-K. Kim, J. Appl. Phys. **104**, 053909 (2008).
[8] V. V. Kruglyak, P. S. Keatley, A. Neudert, M. Delchini, R. J. Hicken, J. R. Childress, and J. A. Katine, Phys. Rev. B **77**, 172407 (2008).
[9] V. E. Demidov, S. O. Demokritov, K. Rott, P. Krzysteczko, and G. Reiss, Phys. Rev. B **77**, 064406 (2008).
[10] J. Topp, J. Podbielski, D. Heitmann, and D. Grundler, Phys. Rev. B **78**, 024431 (2008).
[11] V. Vlaminck and M. Bailleul, Science **322**, 410 (2008).
[12] A. Kozhanov, D. Ouellette, Z. Griffith, M. Rodwell, A. P. Jacob, D. W. Lee, S. X. Wang, and S. J. Allen, Appl. Phys. Lett. **94**, 012505 (2009).
[13] V. E. Demidov, J. Jersch, S. O. Demokritov, K. Rott, P. Krzysteczko, and G. Reiss, Phys. Rev. B **79**, 054417 (2009).
[14] K.-S. Lee, D.-S. Han, and S.-K. Kim, Phys. Rev. Lett. **102**, 127202 (2009).
[15] S.-M. Seo, K.-J. Lee, H. Yang, and T. Ono, Phys. Rev. Lett. **102**, 147202 (2009).
[16] V. E. Demidov, J. Jersch, K. Rott, P. Krzysteczko, G. Reiss, and S. O. Demokritov, Phys. Rev. Lett. **102**, 177207 (2009).
[17] C. Mathieu, V. T. Synogatch, and C. E. Patton, Phys. Rev. B **67**, 104402 (2003).
[18] K. Perzlmaier, G. Woltersdorf, and C. H. Back, Phys. Rev. B **77**, 054425 (2008).
[19] R. W. Damon and J. R. Eshbach, J. Phys. Chem. Solids **19**, 308 (1961).
[20] S. O. Demokritov and V. E. Demidov, IEEE Trans. Magn. **44**, 6 (2008).
[21] B. A. Kalinikos, IEE Proc., Part H: Microwaves, Opt. Antennas **127**, 4 (1980).
[22] S. O. Demokritov, A. A. Serga, A. Andre, V. E. Demidov, M. P. Kostylev, B. Hillebrands, and A. N. Slavin, Phys. Rev. Lett. **93**, 047201 (2004).
[23] O. Büttner, M. Bauer, S. O. Demokritov, B. Hillebrands, Y. S. Kivshar, V. Grimalsky, Yu. Rapoport, and A. N. Slavin, Phys. Rev. B **61**, 11576 (2000).
[24] T. Schneider, A. A. Serga, C. Sandweg, and B. Hillebrands, *Abstracts of the 52nd Annual Conference on Magnetism and Magnetic Materials*, Tampa, Florida, 2007, No. ER-05.